The Probe-Insertion Technique for the Detection of Limit Cycles in Power Systems

F. Bizzarri, *Senior Member, IEEE*, A. Brambilla, *Member, IEEE*, F. Milano, *Fellow, IEEE*

***Abstract*— The paper proposes a technique to accurately and efficiently locate periodic steady-state solutions of electric power systems. This technique is based on an enhanced version of the time-domain shooting method (TDSM) and the probe-insertion technique (PIT). The latter has been successfully applied to low-power electronic circuits but it is innovative for the study of electro-mechanical steady-state periodic behaviour of power systems. With this aim, the paper discusses the inherent criticalities of the conventional formulation of power system models (PSMs). Then, a novel formulation is proposed to accommodate the hypotheses and mathematical requirements of the TDSM and PIT. The effectiveness and numerical efficiency of the proposed model and technique are discussed through two case studies based on the IEEE 14-bus and WSCC 9-bus systems.**

***Index Terms*— Hopf bifurcation, limit cycle, Floquet multipliers, shooting method, probe-insertion technique.**

I. Introduction

The mechanism and the physical causes that lead to the birth of limit cycles in power systems have been object of intense research in the last three decades [1]–[5]. However, existing literature mainly focuses on the detection of Hopf bifurcations, which can be tackled through the analysis of stationary points and parametric small-signal stability analysis [6]–[9]. Existing literature does not focus on the systematic determination of generic limit cycles. On the other hand, in other branches of electrical engineering research, the study of oscillators and limit cycles has been defined and formalized in a systematic way (see, for instance [10]–[13] and references therein).

Relevant techniques proposed in the last three decades to determine periodic solutions of power system models (PSMs) can be found in [14]–[20]. Most references above describe small systems, and modelling issues are solved using *ad hoc* formulations. In [15], [17], the authors define the properties of limit cycles using a dynamic system reduction based on the center manifold. This approximation captures the behavior of the system in a *neighborhood* of the equilibria but does not define the precise trajectory of the limit cycle.

Federico Bizzarri and Angelo Brambilla are with DEIB, Politecnico di Milano, Milano, Italy. E-mail: {federico.bizzarri, angelo.brambilla}@polimi.it Federico Bizzarri is also with the Advanced Research Center on Electronic Systems for Information and Communication Technologies E. De Castro (ARCES), University of Bologna, Italy. Federico Milano is with the UCD School of Electrical and Electronic Engineering, University College Dublin, Belfield, Dublin 4, Ireland.

A more general approach to identify the trajectories of unstable limit cycles is given in [18] and [20]. In these references, the authors compute trajectories iteratively departing from points *inside* and *outside* the stable manifold of the limit-cycle. The trajectory of the unstable limit-cycle is then determined through the interpolation among those trajectories. The major drawback of this technique is the poor computational efficiency (since it is basically a trial-and-error technique) and, more sensibly, the difficulty to define *a priori* which points are inside or outside the stable manifold of the limit cycle.

In this paper, the formalism of two well-assessed techniques, namely the time-domain shooting method (TDSM) [21], [22] and probe-insertion technique (PIT) [23], [24], are applied to the systematic determination of limit cycles in power systems. Limit cycles (stable and unstable) can be originated by both super- and sub-critical Hopf bifurcations or by different mechanisms such as fold or flip bifurcations [25]. Furthermore, limit cycles corresponding to non-self-sustained oscillations can be detected too. They can be found in periodically driven systems, e.g., power system oscillations caused by wind power fluctuations [5].

The TDSM and PIT require that the power system differential algebraic equations (DAEs) are written in a form suitable for the identification of limit cycles by resorting to the sensitivity of the evolution of the system state variables with respect to their initial conditions. In particular, the system fundamental matrix and the monodromy matrix are two key ingredients [26]. With this aim, the paper first discusses why the conventional formulation of power system synchronous machine models and the use of a synchronous reference for the machine rotor speeds and angles has to be revised to allow applying the TDSM and thus PIT. In fact, the conventional formulation presents a "non-physical" singularity in the Jacobian matrix of the Newton iteration scheme used to numerically solve the boundary value problem (BVP) which is the core of the TDSM and hence of the PIT. The presence of this singularity prevents the use of TDSM. This is one of the main aspects considered in the paper and the proposed reformulation of the PSM solves this problem.

The TDSM to locate limit cycles consists in the solution of a BVP with periodic constraints through an iterative scheme suitable for the solution of systems of algebraic nonlinear equations, e.g., the Newton method. If the limit cycle is the periodic steady-state solution of an autonomous system, the Jacobian matrix of the nonlinear algebraic system to be solved exhibits a null eigenvalue and hence it is singular. In this case, the BVP must be augmented with a proper phase condition to remove such a singularity [25]. On the contrary, if the system

is non-autonomous, the Jacobian matrix is full rank. If the classical formulation of the PSM is considered, i.e., generator speeds are relative to a constant synchronous reference, the aforementioned Jacobian matrix is characterized by one additional null eigenvalue; rank-2 and rank-1 deficiencies are thus observed in the autonomous and non-autonomous case, respectively.

Examples can be found in the literature where the aforementioned limitations are not encountered. For instance, in [14] and [19], the authors determine the steady-state solution of a very simple PSM composed of a single machine connected to an infinite bus. The latter provides a phase reference frame that avoids the singularity of the Jacobian matrix. However, the infinite bus model is not appropriate for real-world PSMs.

The paper shows how power system DAEs can be properly reformulated without modifying their inherent meaning in such a way that the TDSM and the PIT can be successfully applied to a system of arbitrary size to locate limit cycles in the system state space. In particular, the proposed enhanced model yields a suitable full-rank bordered Jacobian matrix and hence the iterative Newton scheme can safely converge [27]. The proposed approach relies on a *generalization* of the well-known concept of center of inertia (COI) [28] and, thus, it can be easily implemented in existing power system simulators.

The contributions of the paper are twofold:

1) The TDSM is reviewed and it is highlighted why the standard formulation of PSM does not allow locating periodic steady-state solutions through the TDSM. It is shown how the aforementioned formulation issue can be solved through a matrix-bordering technique based on a generalization of the concept of COI.
2) A systematic approach, namely the PIT, is applied to determine both stable and unstable limit cycles exhibited by the PSM. The determination of the latter is important as they provide insights on the boundary of the region of attraction of the stable equilibrium point [18], [20]. With respect to other techniques proposed in the literature, the PIT provides the exact trajectory of an unstable limit cycle that, as shown in Sec. V-B, is not necessarily a "simple" curve.

The paper is organized as follows. Section II introduces in details the TDSM, which is the basis of the PIT discussed in Section III. Section IV is devoted to the power systems transient stability model; some inherent drawbacks of the conventional model are presented and overcome to accommodate the assumptions and mathematical requirements of the TDSM. Section V illustrates the proposed model and technique through two well-known test systems, namely the IEEE 14-BUS and the WSCC 9-BUS networks. Finally, Section VI draws conclusions and indicate future work directions.

II. The time-domain shooting method

A. Outlines

The TDSM allows solving a BVP as a small number of simpler initial value problems (IVPs) [21], [22]. In general, an n-th order ordinary differential equation (ODE) allows setting n independent boundary conditions – these can be initial conditions (as in IVPs), final conditions, or a mix of the two. To clarify things out, let us consider the following ODE

$$\dot{\boldsymbol{z}} = \boldsymbol{f}(\boldsymbol{z}(t), t) \quad , \tag{1}$$

where $\boldsymbol{z} \in \mathbb{R}^n$ and the time-varying Jacobian matrix of $\boldsymbol{f}$ is denoted by $\boldsymbol{f}_{\boldsymbol{z}}(t)$. Although the PSM is described by a DAE, for the sake of simplicity, we present the TDSM in the ODE case. The conclusions provided in this section can be directly extended to DAEs.

To grasp the idea inherent in the TDSM, it may be useful to recall a classic (simplified) ballistic problem where a gunman has a fixed position of the cannon and of the target (i.e., the boundary conditions) but has freedom in the tilt of the cannon and does not care about the angle of arrival of the cannonball. If a first shot misses the target, the gunner evaluates how much closer or farther the cannon ball gets from his objective and finally adjusts the tilt in order to (hopefully) hit the target with the next shot. The key of the gunman's method is the perturbation of the initial guess of the tilt and the evaluation of the *sensitivity* of the solution (i.e., the arrival position of the cannonball) to this perturbation. The location of limit cycles can be visualized as a variant of the ballistic problem where the gunman is using a boomerang instead of a cannon. In this case, the boundary conditions represent a periodicity constraint.

For the (1) ODE, a boundary condition $\boldsymbol{z}(T_\gamma + t_0) = \boldsymbol{z}(t_0)$ for some time value T_γ defines, if it exists, a T_γ-periodic solution, say $\boldsymbol{\gamma}$, such that $\boldsymbol{\gamma}(t) = \boldsymbol{\gamma}(t + T_\gamma)$.

Any standard numerical integration method can be utilized to find the solution of the IVP from time t_0, with some initial conditions $\boldsymbol{z}(t_0)$, to time $t_0 + T_\gamma$. Moreover, computing at the same time the evolution of the $\boldsymbol{\Phi}(t, t_0)$ state transition matrix associated with (1), i.e., the solution of the *variational equation* [26]

$$\begin{cases} \dot{\boldsymbol{\Phi}}(t, t_0) = \boldsymbol{f}_{\boldsymbol{z}}(t)\boldsymbol{\Phi}(t, t_0) \\ \boldsymbol{\Phi}(t_0, t_0) = \mathbf{1}_n \end{cases} \quad , \tag{2}$$

where $\mathbf{1}_n$ is the $n \times n$ identity matrix, provides the sensitivity of the solution of the IVP problem to its initial conditions. By introducing the *state transition* function $\boldsymbol{\varphi}(\boldsymbol{z}(t_0), t_0, t) \equiv \boldsymbol{z}(t)$ to make evident as the final value reached by the solution of the IVP depends on $\boldsymbol{z}(t_0)$ and t_0, the periodicity condition $\boldsymbol{z}(T_\gamma + t_0) = \boldsymbol{z}(t_0)$ can be reformulated in terms of a non linear algebraic function $\boldsymbol{R}$ to be zeroed as

$$\boldsymbol{R}(\boldsymbol{z}(t_0)) = \boldsymbol{\varphi}(\boldsymbol{z}(t_0), t_0, t_0 + T_\gamma) - \boldsymbol{z}(t_0) = 0 \tag{3}$$

and numerically solved, for example, by using Newton method

$$\boldsymbol{R}_{\boldsymbol{z}(t_0)}(\boldsymbol{z}^i(t_0))(\boldsymbol{z}^{i+1}(t_0) - \boldsymbol{z}^i(t_0)) = -\boldsymbol{R}(\boldsymbol{z}^i(t_0)) \tag{4}$$

where i is the iteration index and the $\boldsymbol{R}_{\boldsymbol{z}(t_0)}(\boldsymbol{z}^i(t_0))$ Jacobian matrix of $\boldsymbol{R}(\boldsymbol{z}(t_0))$ is given by

$$\left.\frac{\partial \boldsymbol{\varphi}(\boldsymbol{z}_0, t_0, t)}{\partial \boldsymbol{z}_0}\right|_{\substack{t = t_0 + T_\gamma \\ \boldsymbol{z}_0 = \boldsymbol{z}_0^i}} - \mathbf{1}_n \equiv \boldsymbol{\Phi}^i(t_0 + T_\gamma, t_0) - \mathbf{1}_n \quad . \tag{5}$$

Using the information embedded in $\boldsymbol{\Phi}(t_0 + T_\gamma, t_0)$, the initial conditions of the IVP are corrected at next step $i + 1$ and a new IVP is solved until the condition $\boldsymbol{z}(T + t_0) = \boldsymbol{z}(t_0)$ is (approximately) met. When this happens, the solution of the

IVP with the *right* initial conditions on the interval $[t_0, t_0 + T_\gamma]$ is $\boldsymbol{\gamma}$. Once the Newton procedure converges towards a periodic solution $\boldsymbol{\gamma}$, the $\boldsymbol{\Phi}(t_0+T, t_0)$ matrix converges towards a matrix $\boldsymbol{\Psi}$ (called *monodromy matrix* or *principal matrix*) whose eigenvalues are the μ_k $(k = 1, ..., n)$ *characteristic multipliers*. If the condition $|\mu_k| \leq 1\ \forall k$ holds, then $\boldsymbol{\gamma}$, which is a limit cycle, is stable.

This is a direct mathematical transposition of the gunman problem: the Jacobian matrix of the Newton scheme represents, through the system state transition matrix, a measure of the sensitivity of the final conditions with respect to initial ones, and the sequence of IVPs, solved for proper different values of the initial conditions, is equivalent to a sequence of tilt adjustments.

As the number of iterations grows, each IVPs is expected to converge to a final value of the trajectory closer and closer to the adjusted initial one. This suggests that the TDSM is not suited to determine unstable limit cycles if the initial conditions of the IVP are not sufficiently close to the repeller. The PIT introduced in Sec. II-B overcomes this limitation.

B. Bordering the Jacobian

An extremely important remark must be done in case (1) represents an *autonomous* system, i.e., it does not explicitly depend on time. In this case, a multiplier of $\boldsymbol{\gamma}$, say μ_1, is equal to 1 [25]. Hence, the Jacobian (5) of the Newton scheme introduced in the previous section tends to be singular as the iterative procedure goes towards $\boldsymbol{\gamma}$ and one cannot safely compute $\boldsymbol{z}_0^{i+1}$ by inverting $\boldsymbol{R}_{\boldsymbol{z}(t_0)}(\boldsymbol{z}^i(t_0))$.[2]

A well known technique to obtain a full rank matrix from a singular one is through the addition of as many extra independent rows and columns as the rank deficiency [27]. This concept is briefly outlined below. Let us assume that $\boldsymbol{B}$ is a rank-1 deficient matrix, as it happens for $\boldsymbol{R}_{\boldsymbol{z}(t_0)}(\boldsymbol{z}^i(t_0))$ when the Newton iteration scheme converges towards $\boldsymbol{\gamma}$. Let $\boldsymbol{\eta}$ be the right eigenvector of $\boldsymbol{B}$ corresponding to the null eigenvalue, i.e., $\boldsymbol{B}\boldsymbol{\eta} = 0$. $\boldsymbol{\eta}$ spans the null space of $\boldsymbol{B}$ and is orthogonal to the image of $\boldsymbol{B}^{\mathrm{T}}$.
If $\boldsymbol{B}$ is bordered with an extra row and column as follows

$$\boldsymbol{A} = \begin{bmatrix} \boldsymbol{B} & \boldsymbol{\eta} \\ \boldsymbol{\eta}^{\mathrm{T}} & \alpha \end{bmatrix} \quad , \tag{6}$$

where $\alpha \in \mathbb{R}$, one obtains that $\det(\boldsymbol{A}) \neq 0$. In fact, consider $\boldsymbol{A}^{\mathrm{T}}$ which has the same eigenvalues of $\boldsymbol{A}$; if $\boldsymbol{A}^{\mathrm{T}}$ were singular it would admit the $\boldsymbol{\zeta}$ null space that would satisfy

$$\begin{bmatrix} \boldsymbol{B}^{\mathrm{T}} & \boldsymbol{\eta} \\ \boldsymbol{\eta}^{\mathrm{T}} & \alpha \end{bmatrix} \overbrace{\begin{bmatrix} \boldsymbol{\zeta}_1 \\ \zeta_2 \end{bmatrix}}^{\boldsymbol{\zeta}} = \boldsymbol{0} \quad . \tag{7}$$

Consider the condition $\boldsymbol{B}^{\mathrm{T}}\boldsymbol{\zeta}_1 + \boldsymbol{\eta}\zeta_2 = \boldsymbol{0}$. Since $\boldsymbol{\eta}$ is orthogonal to the image of $\boldsymbol{B}^{\mathrm{T}}$, it can be satisfied only when $\boldsymbol{\zeta}_1 = \boldsymbol{\eta}$ and $\zeta_2 = 0$ but this implies $\boldsymbol{\eta}^{\mathrm{T}}\boldsymbol{\zeta}_1 = \boldsymbol{\eta}^{\mathrm{T}}\boldsymbol{\eta} \neq 0$ and hence Eq. (7) is not satisfied. This concludes the simple proof that bordering the $\boldsymbol{B}$ matrix with its null space $\boldsymbol{\eta}$ removes its singularity.

From a practical point of view, to solve the problem (3) for an autonomous system, one must include a new equation (involving of course a new unknown). The new equation must not modify the dynamics of the system. This is typically achieved by introducing a *phase condition* $q(\boldsymbol{z}(t_0), T_\gamma) = 0$ that removes the singularity and introduces the unknown T_γ period among the unknowns [25]. The nonlinear algebraic function (3) becomes $\boldsymbol{R}(\boldsymbol{z}(t_0), T_\gamma)$.

In this way, the Jacobian matrix of the Newton scheme associated with the enlarged problem becomes

$$\begin{bmatrix} \boldsymbol{R}_{\boldsymbol{z}(t_0)} & \dfrac{\partial \boldsymbol{R}}{\partial T_\gamma} \\ \nabla^{\mathrm{T}}_{\boldsymbol{z}(t_0)} q & \dfrac{\partial q}{\partial T_\gamma} \end{bmatrix} \quad , \tag{8}$$

where $\nabla^{\mathrm{T}}_{\boldsymbol{z}(t_0)} q$ is the gradient of the scalar function $q(\boldsymbol{z}(t_0), T_\gamma)$ computed with respect to $\boldsymbol{z}(t_0)$. The resulting bordering is quite different from (6) and, to remove the singularity, the following conditions have to be satisfied:

C1. $\dfrac{\partial \boldsymbol{R}}{\partial T_\gamma}$ belongs to a subspace spanned *also* by the null space of $\boldsymbol{R}_{\boldsymbol{z}(t_0)}$

C2. $\nabla^{\mathrm{T}}_{\boldsymbol{z}(t_0)} q \cdot \dfrac{\partial \boldsymbol{R}}{\partial T_\gamma} \neq 0.$

Since it can be shown that the right eigenvector of $\boldsymbol{\Psi}$ associated to μ_1 is $\boldsymbol{f}(\boldsymbol{z}(t_0)) \equiv \boldsymbol{u}_1$ [26], a typical choice for q is the constraint imposing that the correction vector $\boldsymbol{z}^{i+1}(t_0) - \boldsymbol{z}^i(t_0)$ is orthogonal to $\boldsymbol{f}(\boldsymbol{z}^i(t_0))$ [29], [30]. In this way, if the Newton scheme converges to the *right* set of initial conditions and period of the limit cycle, it can be shown that

$$\frac{\partial \boldsymbol{R}}{\partial T_\gamma} = \nabla_{\boldsymbol{z}(t_0)} q = \boldsymbol{u}_1 \quad . \tag{9}$$

If the periodic solution $\boldsymbol{\gamma}$ is characterized by more than one unitary multiplier, i.e., the Jacobian of the Newton scheme has more than one null eigenvalue, a single phase condition is no longer sufficient. In this case, further bordering equations are required, as discussed in the following sections.

III. The probe-insertion technique

The PIT, originally used in harmonic balance, i.e., in the frequency domain [31]–[33], is a valid tool to extend the application of the TDSM to power systems. A time domain version of the PIT was recently proposed in [23], [24]. The remainder of this section shows how to use the PIT to reliably locate limit cycles in the PSM.

To illustrate the basic idea underpinning the PIT, it is assumed that the generic dynamic system described by (1) is autonomous and admits a stable or unstable $\boldsymbol{\gamma}$ periodic solution whose period is T_γ. Then the coefficients of the real Fourier expansion of a component of $\boldsymbol{\gamma}$ can be determined as

$$\begin{aligned} v_R &= \frac{2}{T_\gamma} \int_{t_0}^{t_0+T_\gamma} \cos(\omega_\gamma \tau) \boldsymbol{r}^{\mathrm{T}} \boldsymbol{\gamma}(\tau) d\tau \\ v_I &= \frac{2}{T_\gamma} \int_{t_0}^{t_0+T_\gamma} \sin(\omega_\gamma \tau) \boldsymbol{r}^{\mathrm{T}} \boldsymbol{\gamma}(\tau) d\tau \end{aligned} \quad , \tag{10}$$

[2] Actually, only when $\boldsymbol{R}_{\boldsymbol{z}(t_0)}(\boldsymbol{z}^{\bar{\imath}}(t_0)) = \boldsymbol{\Psi} - \boldsymbol{1}_n$ the Jacobian matrix of the Newton scheme is singular. This happens for the (ideal) final iteration step $\bar{\imath}$. Nevertheless, from a numerical standpoint, the condition number of $\boldsymbol{R}_{\boldsymbol{z}(t_0)}(\boldsymbol{z}^i(t_0))$ increases as i tends towards $\bar{\imath}$. Thus inverting $\boldsymbol{R}_{\boldsymbol{z}(t_0)}(\boldsymbol{z}^i(t_0))$ becomes an issue as i increases.

where $\omega_\gamma = {}^{2\pi}/_{T_\gamma}$ and $\boldsymbol{r}$ is a selector, i.e., a column vector whose entries are all null but one, equal to 1, which corresponds to the considered component of $\boldsymbol{\gamma}$. Let us rewrite (1) as

$$\dot{\boldsymbol{z}} = \boldsymbol{f}(\boldsymbol{z}(t)) + \boldsymbol{r}[y_R \cos(\omega_p t) + y_I \sin(\omega_p t)] \quad , \tag{11}$$

and assume that, before perturbing the system, $y_R = y_I = 0$ and $\omega_p = {}^{2\pi}/_{T_p} > 0$. Then, let us apply the following modelling choices:

- a coefficient of a component of $\boldsymbol{\gamma}$, e.g., v_R, is *slightly* perturbed;
- y_I and T_γ are kept constant; and
- v_I is free to vary.

Other choices of perturbed, constant and free variables are possible, but these do not alter the results of the PIT.[3] Then, an adjusted y_R can be identified such that (11) admits a periodic solution that can be viewed as a small perturbation of γ. In practice, the periodic trajectory can be obtained by solving a BVP defined by (11) augmented by

$$\dot{\kappa}_R = \frac{2}{T_\gamma} \cos(\omega_\gamma t) \boldsymbol{r}^{\mathrm{T}} \boldsymbol{z}(t) \quad , \tag{12}$$

with $y_I = 0$, $\omega_p = \omega_\gamma$ and with the boundary conditions $\boldsymbol{z}(T_\gamma + t_0) = \boldsymbol{z}(t_0)$ and $\kappa_R(t_0 + T_\gamma) - \kappa_R(t_0) = v_R + \Delta v_R$.[4] This BVP, whose unknowns are $\boldsymbol{z}_0$ and y_R, can be solved through the TDSM. According to Section II, the Jacobian matrix at the $i-$th step of the Newton iterative scheme used to solve the BVP (11)-(12) is

$$\begin{bmatrix} \boldsymbol{B} & \boldsymbol{\rho}_{y_R} \\ \boldsymbol{\chi}_{v_R} & \alpha_{y_R} \end{bmatrix} \quad , \tag{14}$$

where

$$\begin{aligned} \boldsymbol{B} &= \boldsymbol{R}_{\boldsymbol{z}(t_0)} \\ \boldsymbol{\rho}_{y_R} &= \frac{\partial \boldsymbol{\varphi}(\boldsymbol{z}(t_0), t_0, t_0 + t, y_R, y_I, \omega_p)}{\partial y_R} \\ \boldsymbol{\chi}_{v_R} &= \boldsymbol{r}^{\mathrm{T}} \frac{2}{T_p} \int_{t_0}^{t_0 + T_\gamma} \boldsymbol{\Phi}^i(t_0 + T_p, t_0) \cos(\omega_p \tau) d\tau \\ \alpha_{y_R} &= \boldsymbol{r}^{\mathrm{T}} \frac{2}{T_p} \int_{t_0}^{t_0 + T_\gamma} \boldsymbol{\rho}_{\boldsymbol{y_R}} \cos(\omega_p \tau) d\tau \end{aligned} \quad , \tag{15}$$

evaluated for $t = t_0 + T_\gamma$, $\boldsymbol{z}_0 = \boldsymbol{z}_0^i$ and $y_R = y_R^i$.

As far as the computation of $\boldsymbol{\rho}_{y_R}$ is concerned, evaluating the partial derivative of (11) with respect to y_R, leads to

$$\dot{\boldsymbol{\rho}}_{y_R} = \boldsymbol{f}_{\boldsymbol{z}} \boldsymbol{\rho}_{y_R} + \boldsymbol{r} \cos(\omega_p t) \quad . \tag{16}$$

Thus, since $\boldsymbol{\rho}_{y_R}(t_0) = \frac{\partial \boldsymbol{z}_0(y_R)}{\partial y_R} = \boldsymbol{0}$, $\boldsymbol{\rho}_{y_R}$ can be obtained by solving (16) along with (11).

[3]The PIT performance, basically in terms of converge rate of the algorithm, is sensitive to the choice of $\boldsymbol{r}$ and to the parameters to be altered, fixed, let free and adjusted. A detailed discussion on these aspects is beyond the scope of this work. The interested reader can refer to [33].

[4]Equation (12) together with the last mentioned boundary condition yield the integral constraint originally reported in Eq. (1) of [24]. The formulation of this integral constraint in differential form allows us to solve (12) along with (11) and obtain

$$\kappa_R(t_0 + T_\gamma) - \kappa_R(t_0) = \int_{t_0}^{t_0 + T_\gamma} \cos(\omega_\gamma t) \boldsymbol{r}^{\mathrm{T}} \boldsymbol{z}(t) dt \quad . \tag{13}$$

The PIT is particularly useful to determine unstable $\boldsymbol{\gamma}$ limit cycles of (11) with $y_R = y_I = 0$, starting from a limit cycle with non null y_R and/or y_I. To explain this point, let $\dot{\boldsymbol{z}} = \boldsymbol{f}(\boldsymbol{z})$ exhibit a $\boldsymbol{\gamma}$ unstable limit cycle. The PIT is applied as follows.

- `Step 1`. Identify an initial guess for ω_p. For limit cycles originated by a Hopf bifurcation of an equilibrium E_0 the eigenvalues of the $\boldsymbol{f}_{\boldsymbol{z}}$ system Jacobian at E_0 identify the angular frequencies related to the imaginary part of these eigenvalues. Such frequencies are good initial guesses for ω_p.
- `Step 2`. Select the component of $\boldsymbol{z}$ to be used to insert the forcing term ruled by y_R, y_I and ω_p, and set $\boldsymbol{r}$ accordingly. Mechanisms to identify a suitable component of $\boldsymbol{z}$ were suggested in [24], [33].
- `Step 3`. Set $y_I = 0$, $v_R = \Delta v_R$ (with $|\Delta v_R| \ll 1$) and $y_R^{\mathrm{old}} = 0$.
- `Step 4`. Solve the PIT-BVP to find a value of y_R and a set of initial conditions $\boldsymbol{z}_0$ that correspond to a periodic solution of $\dot{\boldsymbol{z}} = \boldsymbol{f}(\boldsymbol{z}(t)) + \boldsymbol{r} y_R \cos(\omega_p t)$ with $v_R = \frac{2}{T_p} \int_{t_0}^{t_0 + T_p} \cos(\omega_p \tau) \boldsymbol{r}^{\mathrm{T}} \boldsymbol{z}(\tau) d\tau$.
- `Step 5`. If $y_R^{\mathrm{old}} y_R < 0$ fix $\bar{v}_R = v_R$ and go to `Step 6`. Otherwise, set $y_R^{\mathrm{old}} = y_R$, $v_R = v_R + \Delta v_R$ and go to `Step 4`.
- `Step 6`. Fix $y_R = 0$ and solve the PIT-BVP to find out a value of ω_p and a set of initial conditions $\boldsymbol{z}_0$ that correspond to a periodic solution of $\dot{\boldsymbol{z}} = \boldsymbol{f}(\boldsymbol{z}(t))$ with $\bar{v}_R = \frac{2}{T_p} \int_{t_0}^{t_0 + T_p} \cos(\omega_p \tau) \boldsymbol{r}^{\mathrm{T}} \boldsymbol{z}(\tau) d\tau$. In this final step, a proper $\boldsymbol{\rho}_{\omega_p}$ and α_{ω_p} must be used in Eq. (14) instead of $\boldsymbol{\rho}_{y_R}$ and α_{y_R}, respectively.[5]

After completing `Step 6`, $\boldsymbol{B}$ in (14) exhibits one null eigenvalue and the vectors $\boldsymbol{\rho}_{\omega_p}$ and $\boldsymbol{\chi}_{v_R}$ represent a bordering of the Jacobian of the Newton iterative scheme used to apply the PIT.

We recall that since the PIT is applied to identify a limit cycle of power systems, the BVP inherent to the PIT must be further augmented by using the bordering based on the center of inertia as detailed in Sec. IV-C and Sec. IV-D.

Information on the stability of the limit cycle detected by using the PIT can be derived by computing a scalar G defined as:

$$G = \alpha_{y_R}^{-1} [1 - \boldsymbol{\chi}_{v_R} (\boldsymbol{\rho}_{y_R} \boldsymbol{\chi}_{v_R} - \alpha_{y_R} \boldsymbol{B}) \boldsymbol{\rho}_{y_R}] \quad . \tag{18}$$

If $G < 0$ after completing `Step 6`, then the limit cycle is stable, otherwise it is unstable. The interested reader can refer to [24] for further details on this point.

IV. Revisited Power System Model

This section presents a transient stability model of power systems using a formal and slightly unconventional notation.

[5]An efficient implementation of the PIT should compute in parallel $\boldsymbol{\rho}_{y_R}$, $\boldsymbol{\rho}_{y_I}$, $\boldsymbol{\rho}_{\omega_p}$, $\boldsymbol{\chi}_{v_R}$, $\boldsymbol{\chi}_{v_I}$, α_{y_R}, α_{y_I} and α_{ω_p}. This can be easily done by solving the forward sensitivity problem [34], associated with (11)-(12) and

$$\dot{\kappa}_I = \frac{2}{T_\gamma} \sin(\omega_\gamma t) \boldsymbol{r}^{\mathrm{T}} \boldsymbol{z}(t) \quad , \tag{17}$$

not only with respect to the initial conditions (i.e., the variational equation) but also with respect to the parameters y_R, y_I and ω_p. This is useful to design sweeping strategies other than that described in `Step 1` - `Step 6` of the algorithm described in the following.

This notation allows applying the TDSM described in Section II and poses the basis for the PIT discussed in Section III.

A. Outlines of standard power system models

The standard electro-mechanical equation of the rotor speed of synchronous machines can be written as follows:

$$\boldsymbol{M}\dot{\boldsymbol{\omega}}+\boldsymbol{D}(\boldsymbol{\omega}-\omega_0)-\boldsymbol{P}_m(\boldsymbol{\omega},\boldsymbol{x},\boldsymbol{y})+\boldsymbol{P}_e(\boldsymbol{\delta},\boldsymbol{x},\boldsymbol{v},\boldsymbol{\theta},\boldsymbol{y})=\boldsymbol{0} \quad (19)$$

where the dependence on time is dropped to gain compactness. Being M the number of machines, symbols in (19) have the following meaning:

- $\boldsymbol{\omega}(t) \in \mathbb{R}^M$ are the rotor speeds of the machines;
- $\omega_0 \in \mathbb{R}$ is the reference synchronous frequency;
- $\boldsymbol{\delta}(t) \in \mathbb{R}^M$ are the rotor angles of the machines;
- $\boldsymbol{M} \in \mathbb{R}^{M\times M}$ is a diagonal matrix whose entries model the inertia constants of the machines;
- $\boldsymbol{x}(t) \in \mathbb{R}^N$ are the N state variables of the PSM ($\boldsymbol{\omega}$ and $\boldsymbol{\delta}$ excluded) that may influence the dynamics of the machines,
- $\boldsymbol{y}(t) \in \mathbb{R}^S$ are all the algebraic variables of the PSM but $\boldsymbol{v}$ and $\boldsymbol{\theta}$;
- $\boldsymbol{D} \in \mathbb{R}^{M\times M}$ is a diagonal matrix whose entries d_{jj} (for $j = 1,\dots,M$) model the damping factor of the machines;
- $\boldsymbol{v}(t) \in \mathbb{R}^P$ and $\boldsymbol{\theta}(t) \in \mathbb{R}^P$ are bus voltages and phases, respectively, where P are the number of buses;
- $\boldsymbol{P}_m(\boldsymbol{\omega},\boldsymbol{x},\boldsymbol{y}) \in \mathbb{R}^M$ is the mechanical power regulated by controllers depending on $\boldsymbol{\omega}$, $\boldsymbol{x}$, and $\boldsymbol{y}$;
- $\boldsymbol{P}_e(\boldsymbol{\delta},\boldsymbol{x},\boldsymbol{v},\boldsymbol{\theta},\boldsymbol{y}) \in \mathbb{R}^M$ is the electrical power exchanged by machines.

The DAEs ruling the dynamics of the whole PSM are defined as:

$$\begin{cases} \dot{\boldsymbol{\delta}} - \Omega\,(\boldsymbol{\omega}-\omega_0) = \boldsymbol{0} \\ \boldsymbol{M}\dot{\boldsymbol{\omega}}+\boldsymbol{D}(\boldsymbol{\omega}-\omega_0)-\boldsymbol{P}_m(\boldsymbol{\omega},\boldsymbol{x},\boldsymbol{y})+\boldsymbol{P}_e(\boldsymbol{\delta},\boldsymbol{x},\boldsymbol{v},\boldsymbol{\theta},\boldsymbol{y})=\boldsymbol{0} \\ \dot{\boldsymbol{x}} - \boldsymbol{F}\,(\boldsymbol{\delta},\boldsymbol{\omega},\boldsymbol{x},\boldsymbol{v},\boldsymbol{\theta},\boldsymbol{y}) = \boldsymbol{0} \\ \boldsymbol{G}\,(\boldsymbol{\delta},\boldsymbol{\omega},\boldsymbol{x},\boldsymbol{v},\boldsymbol{\theta},\boldsymbol{y}) = \boldsymbol{0} \end{cases} \quad (20)$$

where $\boldsymbol{F}(\cdot)$ and $\boldsymbol{G}(\cdot)$ complete the model of the machines, and Ω is the base synchronous frequency in rad/s. $\boldsymbol{F}(\cdot)$ accounts for regulators and other dynamics included in the system, while $\boldsymbol{G}(\cdot)$ models algebraic constraints such as lumped models of transmission lines, transformers and static loads. Note that the standard power flow equations are a subset of $\boldsymbol{G}(\cdot)$ and are used to compute a stationary solution. In particular, power flow equations involve $\boldsymbol{v}$ and $\boldsymbol{\theta}$ only. As detailed in [35], the power flow (PF) solution (hereinafter denoted with the subscript PF) is used to determine the initial equilibrium point of (20).

To better understand the discussion provided later on in this section, it is important to note that $\boldsymbol{P}_e(\cdot)$ does not singularly depend on $\boldsymbol{\theta}_{\text{PF}}$ and $\boldsymbol{\delta}_{\text{PF}}$ but on their difference $\boldsymbol{\theta}_{\text{PF}} - \boldsymbol{\delta}_{\text{PF}}$ only. This means that a shifted set of variables $\boldsymbol{\delta}' = \boldsymbol{\delta}_{\text{PF}} + \bar{\delta}$ ($\bar{\delta} \in \mathbb{R}$) still satisfy (20).

From the viewpoint of dynamical systems theory, the consideration above means that the stationary PSM solution is not an *isolated equilibrium* but it is embedded in a *continuum of equilibria* [36]. This is confirmed by an *always null eigenvalue* of the Jacobian matrix of the PSM linearized at any PF solution [35]. This should not surprise as the classical PSM aims at representing the envelope of the *actual* system dynamics through a PF solution. In other words, the *periodic steady-state* solution at the fundamental frequency with a *constant* envelope is actually represented as a *constant* PF solution playing the role of a *stationary solution*. All together, the admissible shifted PF solutions represent a one-dimensional manifold Γ (parametrized by $\bar{\delta}$) in the phase space.[6] A projection of this manifold in the $M-$dimensional subspace of the state variables $\boldsymbol{\delta}$ is the locus of point $\boldsymbol{\delta}' = \boldsymbol{\delta}_{\text{PF}} + \bar{\delta}$.

B. From polar to rectangular coordinates

Since the objective is the location of periodic steady-state solutions of the PSM, *periodic orbits must be represented as such*. This apparently trivial statement is actually not generally satisfied by the standard formulation of PSM in polar coordinates. A recast of (20) in rectangular coordinates is required since the TDSM is based on the formulation of a BVP with periodic constraints. In fact, it can happen that a limit cycle in rectangular coordinates is a diverging trajectory in polar coordinates having a phase angle arbitrary increasing in time. To clarify this important point, let us consider the following autonomous polar oscillator example

$$\begin{cases} \dot{\rho} + \rho - \rho_0 = 0 \\ \dot{\delta} - \Omega\,(\omega-\omega_0) = 0 \end{cases}, \quad (21)$$

whose steady-state solution, i.e., $\rho(t) = \rho_0$ and $\delta(t) = \Omega\,(\omega-\omega_0)\,t$ is unbounded (the initial condition $\delta(t_0) = 0$ is assumed). However, if (21) is recast using the following

$$\begin{array}{l} c = \rho\cos(\delta) \\ s = \rho\sin(\delta) \end{array}, \quad (22)$$

i.e., using rectangular coordinates, the system exhibits a trivial periodic solution.

PSM can exhibit a similar behavior as (21). In fact, there can exist steady-state solutions of (20) such that $\boldsymbol{\omega}-\omega_0 = \Delta\boldsymbol{\omega} \neq \boldsymbol{0}$ is a *constant* vector and $\dot{\boldsymbol{\omega}} = 0$. This can happen, for example, as a consequence of the droop control of primary frequency regulation. In this case, as t increases, $\boldsymbol{\delta}(t)$ linearly tends to ∞ and so does $\boldsymbol{\theta}(t)$. Nevertheless, the rectangular coordinates of voltage phasors, namely, $\boldsymbol{v}_{\text{q}}(t)$ and $\boldsymbol{v}_{\text{d}}(t)$ components of $(\boldsymbol{v},\boldsymbol{\theta})$, are periodic time varying functions describing a close trajectory. Thus the trajectory is divergent in the polar coordinate frame and periodic in rectangular coordinates.

To avoid the divergent behavior of polar coordinates, the first equation of (20) is recast using a rectangular reference frame. Each component δ_j of $\boldsymbol{\delta}$ is projected onto the unit circle in $\mathbb{R}^2$ using the transformation (22) with $\rho = 1$, i.e., $(\delta_j, 1) \to (c_j, s_j)$. Since there are two new unknowns for each entry of $\boldsymbol{\delta}$, the first equation in (20) is replaced by M pairs of equations. Introducing the vectors $\boldsymbol{c}$ and $\boldsymbol{s}$ storing the state

[6]The *phase space* is the space in which all possible states of a dynamical system are represented. For a DAE the dimension of the phase space is the given by the number of differential variables. In this case such a dimension is $2M + N$.

variables c_j and s_j (for $j = 1, ..., M$), the other equations of (20) are properly modified and the new set of PSM equations

$$\begin{cases} \dot{\boldsymbol{c}} + \Omega\left(\boldsymbol{\Delta}_{\boldsymbol{\omega}} - \omega_o\right)\boldsymbol{s} = \boldsymbol{0} \\ \dot{\boldsymbol{s}} - \Omega\left(\boldsymbol{\Delta}_{\boldsymbol{\omega}} - \omega_o\right)\boldsymbol{c} = \boldsymbol{0} \\ \boldsymbol{M}\dot{\boldsymbol{\omega}} + \boldsymbol{D}(\boldsymbol{\omega} - \omega_0) - \boldsymbol{P}_m(\boldsymbol{\omega}, \boldsymbol{x}, \boldsymbol{y}) + \boldsymbol{P}_e(\boldsymbol{c}, \boldsymbol{s}, \boldsymbol{x}, \boldsymbol{v}, \boldsymbol{\theta}, \boldsymbol{y}) = \boldsymbol{0} \\ \dot{\boldsymbol{x}} - \boldsymbol{F}\left(\boldsymbol{c}, \boldsymbol{s}, \boldsymbol{\omega}, \boldsymbol{x}, \boldsymbol{v}, \boldsymbol{\theta}, \boldsymbol{y}\right) = \boldsymbol{0} \\ \boldsymbol{G}\left(\boldsymbol{c}, \boldsymbol{s}, \boldsymbol{\omega}, \boldsymbol{x}, \boldsymbol{v}, \boldsymbol{\theta}, \boldsymbol{y}\right) = \boldsymbol{0} \end{cases} \tag{23}$$

is obtained, where $\boldsymbol{\Delta}_{\boldsymbol{\omega}}$ is a diagonal matrix whose entries $\boldsymbol{\Delta}_{\boldsymbol{\omega}_{jj}} = \omega_j$, for $j = 1, .., M$.[7]

Let us consider again the one-dimensional manifold Γ introduced in Section IV-A. When dealing with PSM equations in rectangular coordinates, the inherent periodicity of $\boldsymbol{\delta}$ angles makes Γ a closed one-dimensional curve in $\mathbb{R}^{3M+N}$, being $3M + N$ the new dimension of the phase space.

C. On the unit multipliers of the power system model periodic orbits

If the PSM exhibits a periodic (un)stable steady-state solution $\boldsymbol{\gamma}$, originated, for instance, from a Hopf bifurcation of the PF solution, such a *limit cycle* has to be handled with care. As a matter of fact, as it happens for the PF equilibria, $\boldsymbol{\gamma}$ is not an isolated limit cycle but it is embedded in a *continuum of limit cycles* [37]. This occurs since the PSM aims at isolating one of the infinite possible solutions $\boldsymbol{\gamma}$, exactly as it does for the PF ones. Each one of these infinite periodic solutions represents the *periodic modulation* of the constant envelope of the periodic steady-state solution at the fundamental frequency represented as a constant PF solution.

These modulated envelopes differ only by a constant shift of their $\boldsymbol{\delta}$ components and a continuum of periodic solutions is thus often considered as an isolated limit cycle. Among the drawbacks of this modelling approach, if $\boldsymbol{\gamma}$ is a self-sustained limit cycle, i.e., the system is not periodically forced, its monodromy matrix has two unit multipliers. One of them is *trivial*, as discussed in Subsection II-A, but the other one is a direct consequence of the limit cycle *isolation procedure* which is inherent of the PSM. The non-trivial unitary Floquet multiplier is the equivalent of the always null eigenvalue of the Jacobian matrix of the PSM that can be found for any PF solution [35]. If the system is non-autonomous, i.e., there is a periodic external signal forcing it, only the non trivial null multiplier is observed in the monodromy matrix of $\boldsymbol{\gamma}$.

The considerations above pose issues if one aims at locating $\boldsymbol{\gamma}$ through the TDSM since, as shown in Section II-B, unit multipliers correspond to rank deficiency of the Jacobian matrix involved in the Newton scheme used to solve the periodic BVP.

D. Bordering based on the center of inertia

As a first step, in (23), a constant $c_o \in \mathbb{R}$ is added to c_j in all the M pairs of equations ruling the machine dynamics thus obtaining

$$\begin{cases} \dot{\boldsymbol{c}} + \Omega\left(\boldsymbol{\Delta}_{\boldsymbol{\omega}} - \omega_o\right)\boldsymbol{s} = \boldsymbol{0} \\ \dot{\boldsymbol{s}} - \Omega\left(\boldsymbol{\Delta}_{\boldsymbol{\omega}} - \omega_o\right)\left(\boldsymbol{c} + c_o\right) = \boldsymbol{0} \end{cases}, \tag{24}$$

where the c_o constant is used only in the detection of $\boldsymbol{\gamma}$ limit cycles through the TDSM and it is set to 0 to solve the PF. An equivalent result is obtained by adding a constant $s_o \in \mathbb{R}$ to the s_j variables.[8]

In this way, the conventional structure of machine models is preserved. When the TDSM is applied, the PSM is integrated in parallel with its variational equations (see Subsection II-A) thus achieving the sensitivity of its trajectories with respect to their initial conditions.

If the system is non-autonomous, the period T_γ is imposed by the time-varying periodic driving function and a phase condition is not needed. If the system is autonomous, a phase condition is introduced to remove the trivial unit multiplier of the monodromy matrix and to identify T_γ.

In both cases, to remove the non-trivial singularity of the Jacobian, induced by the second unit multiplier of the monodromy matrix, a bordering equation is added taking the cue from the COI expression [28] in rectangular coordinates. In particular, the following equation is used

$$q_c(\underbrace{\boldsymbol{c}, \boldsymbol{s}, \boldsymbol{\omega}, \boldsymbol{x}}_{\boldsymbol{z}}, c_o) = \frac{\sum_j M_j \left(c_j(t_0) + c_o\right)}{\sum_j M_j} = 0 \tag{25}$$

where M_j is the inertia constant of the j-th machine, and c_o is updated during the iterations of the Newton scheme used in the TDSM to compute the steady-state solution and, at converge, it isolates a limit cycle among the infinite equivalent ones as discussed in Subsection IV-C.

If in (24) a constant s_o is added to $\boldsymbol{s}$ instead of adding c_o to $\boldsymbol{c}$, one should use

$$q_s(\boldsymbol{c}, \boldsymbol{s}, \boldsymbol{\omega}, \boldsymbol{x}, s_o) = \frac{\sum_j M_j \left(s_j(t_0) + s_o\right)}{\sum_j M_j} = 0 \quad .$$

As far as conditions $C1$ and $C2$ are concerned (see Section II-B), in general, it is not trivial to verify that a chosen bordering equation fulfills them, since $\boldsymbol{\Psi}$ depends on the dynamical equations governing the system and on the specific limit cycle $\boldsymbol{\gamma}$ the monodromy matrix is referred to. The authors have tested (25) for several power systems, including but not limited to the case studies discussed in Section V. The proposed expression for $q_c(\boldsymbol{z}(t_0), c_o)$ revealed suitable in all cases.

V. Case Studies

In this section, the proposed TDSM is applied to two well-known test systems: (i) the IEEE 14-BUS system, which shows a stable limit cycle; and (ii) the WSSC 9-BUS system, which shows an unstable limit cycle coexisting with a stable equilibrium point.

In both examples, a preliminary parametric analysis to determine the occurrence of Hopf bifurcations is solved. With this aim, load power consumption as well as generation active

[7] Further details concerning numerical aspects related to the described variable transformation are provided in Appendix A.

[8] From a practical point of view, because of numerical issues, these equations are modified as described in Appendix A.

power productions are parametrized by means of a scalar loading level λ. Bifurcation analysis of the PF solutions is not a prerequisite to apply neither the TDSM nor the PIT. Such a bifurcation analysis, however, provides a rationale behind the occurrence of limit cycles.

PQ load power consumption is defined as:

$$\begin{aligned} \boldsymbol{p}_L &= \boldsymbol{p}_L^0 (1+\lambda) \\ \boldsymbol{q}_L &= \boldsymbol{q}_L^0 (1+\lambda) \end{aligned} \tag{26}$$

where $\boldsymbol{p}_L^0$ and $\boldsymbol{q}_L^0$ are load base-case active and reactive powers, respectively. In a similar way, PV generator active powers are defined as:

$$\boldsymbol{p}_G = \boldsymbol{p}_G^0 (1+\lambda) \tag{27}$$

where $\boldsymbol{p}_G^0$ are the generator base-case active power productions. The models above are used to define the power flow solution, then machine and regulator variables are initialized according to the operating point.

The reported simulations were performed on INTEL-i7 2.3 GHz personal computer equipped with 16 GByte RAM, running LINUX-MINT.[9]

A. IEEE 14-bus test system

The proposed TDSM was firstly applied to the IEEE 14-BUS test system. Generators are described by fifth and sixth order models with voltage regulators (IEEE type I) and turbine governors. To force the occurrence of Hopf bifurcations and following limit cycles, no power system stabilizer is included in the system. All static and dynamic data can be found in [28].

A sweep of the loading level parameter λ shows that a Hopf bifurcation occurs for $\lambda = \lambda^* \approx 0.2802$. For $\lambda = 0.4$, the eigenvalues lay "well inside" the instability region and a time domain analysis evidences the existence of a stable limit cycle. Since stable limit cycles can be determined using a conventional time domain simulation, the use of the PIT is not strictly necessary. However, the time domain simulation only provide a qualitative information. Then, matrix bordering is still necessary as discussed in Subsection II-B. By observing the imaginary part of the pair of eigenvalues generating the Hopf, we chose a frequency of $1.442\,\mathrm{Hz}$ as initial guess for TDSM. At convergence of the TDSM, the working frequency was $1.430\,\mathrm{Hz}$, that is very close to the initial value. Fig. 1 shows the projection of the orbit on the (V_1, ω_1) plane, where V_1 is the voltage phasor magnitude at bus 1 and ω_1 is the working angular frequency of the generator connected to bus 1.

Finally, we consider the Floquet multipliers, e.g., the eigenvalues of the monodromy matrix, of the obtained stationary solution. By computing and sorting in descending order the moduli of Floquet multipliers, the two largest ones are equal to 1, as expected, since they are due to the autonomous nature of the power system and to the PSM structure as detailed in Subsection IV-C. The third largest Floquet multiplier is equal to 0.986, thus confirming the stability of the periodic orbit shown in Fig. 1.

[9]The proposed methods were implemented in our simulator PAN [38] that can be downloaded from `brambilla.ws.dei.polimi.it`.

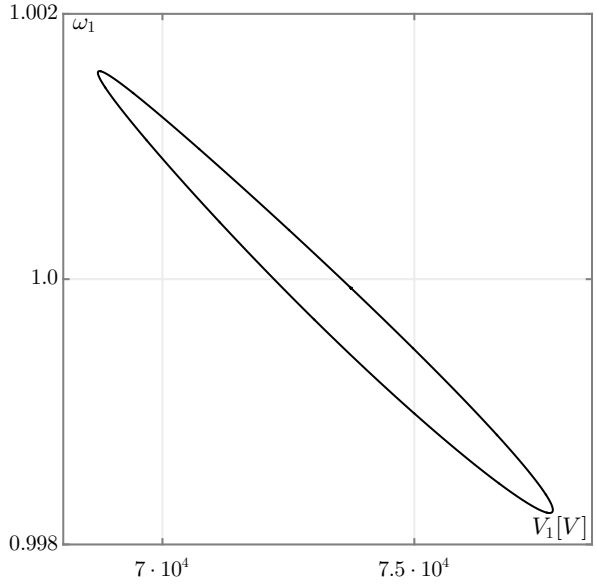

Fig. 1. A projection of the stable limit cycles on the plane (V_1, ω_1) obtained for the overloaded IEEE 14-BUS test system ($\lambda = 0.4$). V_1 is the voltage phasor magnitude at bus 1 voltage and ω_1 is the working angular frequency of the generator connected to bus 1.

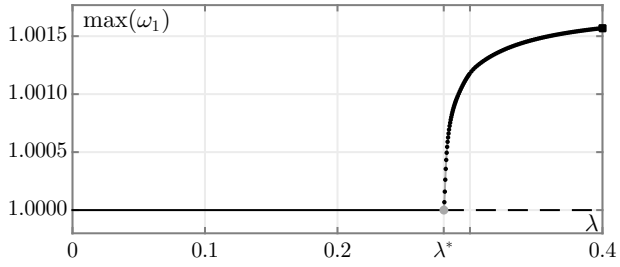

Fig. 2. Bifurcation diagram for the IEEE 14-BUS test system for $\lambda \in [0, 0.4]$. The gray dot represents the super-critical Hopf bifurcation of the PF solution that is stable for $\lambda < \lambda^*$ (black solid line) and unstable for $\lambda > \lambda^*$ (black dashed line). Black dots represent limit cycles originated from the Hopf bifurcation. The square corresponds to the limit cycle depicted in Fig. 1.

The TDSM and the computation of the eigenvalues of the principal matrix required $720\,\mathrm{ms}$ of CPU time; 8 iterations of the Hybrid-Newton method [39] were required to obtain the steady-state solution.

To validate that the limit cycle obtained by resorting to the TDSM for $\lambda = 0.40$ is actually originated by the Hopf bifurcation of the PF solution, we decreased λ from 0.4 to λ^* moving on a discrete grid of values of this parameter and the TDSM was applied at all of these values. Figure 2 shows the bifurcation diagram of ω_1, i.e., the angular speed of the generator connected to bus 1, for each λ value both for the PF solution and the limit cycle. The diagram confirms that the Hopf bifurcation is super-critical and the limit cycle obtained for $\lambda = 0.40$ is originated from such a bifurcation.

B. WSCC 9-bus test system

In this case study, we consider the WSSC 9-BUS 3-machine system described in [40]. Generators are modelled using the d-q axis model and automatic voltage regulators (IEEE type I). The parametric analysis shows that for $\lambda = \lambda^* \approx 1.0571$ the equilibrium point becomes unstable and undergoes a sub-critical Hopf bifurcation. Since the Hopf bifurcation is sub-critical, an interval (λ_-, λ^*) exists such that an unstable limit cycle coexists with the PF solution [25]. This result is local with respect to λ^*. Note that, in this case, the time domain simulation does not help as trajectories cannot fall on the unstable limit cycle.

The steps of the PIT described in Section III are applied after having recast the PSM in rectangular coordinates as discussed in Subsection IV-B. The external signal forcing the system was added to the equations describing the dynamics of the c variable (see (23)) of the machine connected to bus 2. The algorithm starts with $v_R = 10^{-2}$ and $\omega = {}^{4\pi}/_{5}$. In `Step 4` a first limit cycle of the forced system is located corresponding to $y_R = -0.0837$ (see the curve a in Fig. 3).

The procedure continues iterating from `Step 5` to `Step 4` until $v_R = 0.0259$ when y_R becomes positive (c curve in Fig. 3). At each iteration, v_R is increased by 10%. Then `Step 6` is solved and a limit cycle of the autonomous system is obtained for $y_R = y_I = 0$, $v_R = 0.0214$, $v_I = 0.0381$ and $\omega = 2.5424$ (light gray curve in Fig. 3). Evaluating (18), one can find $G = 31.4833 > 0$, i.e., the limit cycle is unstable. This is also confirmed by computing the Floquet multipliers of the periodic orbit. In fact, the magnitude of the largest multiplier is 2.2347.

As discussed in [18], [20], it is important to determine unstable limit cycles as they provide the boundary of the region of attraction of the stable equilibrium point. With respect to other techniques proposed in the literature, the PIT is able to define the exact trajectory of the limit cycle, which, as shown in Fig. 3 is not necessarily a "simple" curve.

The PIT took $14.43\,\mathrm{s}$ CPU time; this time is greater than that of the IEEE 14-BUS case since several TDSM simulations were performed during `Step 4` and `Step 6` of the PIT.

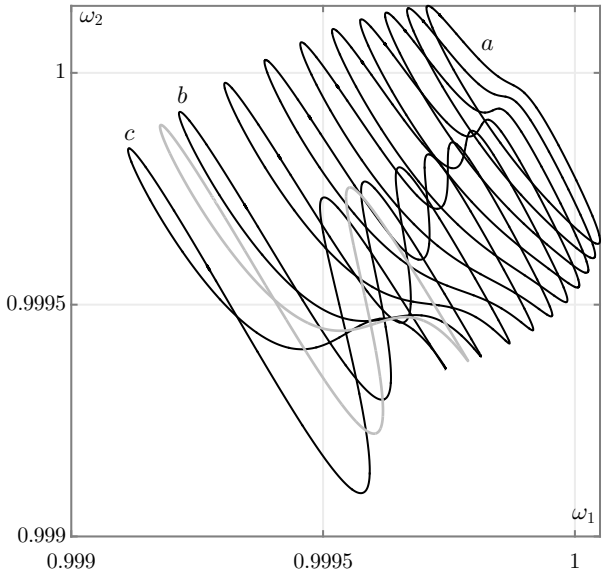

Fig. 3. A projection of the limit cycles obtained with the PIT on the plane (ω_1, ω_2). ω_1 and ω_2 are the rotor speeds of the machines of the WSSC 9-BUS test system connected to bus 1 and 2, respectively. The first limit cycle obtained for $v_R = 10^{-2}$ is labeled with a. The label c corresponds to the last limit cycle obtained for $v_R = 0.0259$. y_R changes sign from negative to positive from the b limit cycle to the c one. The light gray limit cycle is detected at `Step 6` and it corresponds to an unstable periodic steady-state solution of the autonomous systems, i.e., $y_R = y_I = 0$.

VI. Conclusions

The paper shows an application of TDSM and PIT to determine limit cycles in power systems. The main advantage of the proposed technique is the ability to identify both stable and unstable periodic orbits in a unique framework. Moreover, the technique shows a lower computational burden than other techniques proposed in the literature, e.g., [20].

The paper also proposes an unconventional formulation of the power system model to cope with the requirements of the TDSM. The main feature of the proposed model concerns the representation of the speed reference of synchronous machines. This model is basically a generalized center of inertia and involves a recast of the variables to avoid aperiodic drifting of machine angles.

Future works will focus on two directions. The extension of the proposed techniques to power systems with inclusion of hard limits and/or discontinuities on the right hand side of differential equations (see, for example, [4]) appears as a completion of the work presented in this paper. The proposed generalization of the center of inertia indicates that a proper reformulation of synchronous machine equations allows applying techniques that are well-assessed in circuit analysis. Rethinking power system models based on rigorous formalism appears as a challenging field of research.

Appendix A

The projection of each component δ_j of $\boldsymbol{\delta}$ on the unit circle in $\mathbb{R}^2$, using the transformation (22) with $\rho = 1$, i.e., $(\delta_j, 1) \to (c_j, s_j)$, must be handled with care if one aims at numerically solving (23). As matter of fact linear multi-step integration methods, which are largely used to solve non-linear stiff DAEs warp time and introduce additional damping factors [41]. This means that, from a numerical point of view, focusing on the $j-$th machine, the dynamics of c_j and s_j is ruled by the following equations

$$\begin{cases} \dot{c}_j + \lambda_j^c c_j + s_j \Omega \left(\omega_j - \omega_o\right) = 0 \\ \dot{s}_j + \lambda_j^s s_j - c_j \Omega \left(\omega_j - \omega_o\right) = 0 \end{cases}, \tag{28}$$

where λ_j^c and λ_j^s are real parameters depending on the chosen integration method. It is worth realizing that, at the PF equilibrium, i.e., for $\omega_j = \omega_o$, the state variables c_j and s_j do not remain constant but collapse towards $(0, 0)$ as far as the simulation time increases. To avoid this one can use the dynamical equation $\dot{\rho}_j + \rho_j - 1 = 0$. In this way, the numerical integration procedure provides the steady-state solution $\rho_j = 1$ and δ_j is guaranteed to belong to the unit circle, thus satisfying $c_j^2 + s_j^2 = 1$. In other words, ρ_j is *not assumed* to be 1 but it is

forced to be so. In this way, the equation ruling the dynamics of δ_j becomes

$$\begin{cases} \dot{c}_j + c_j + s_j\Omega\left(\omega_j - \omega_o\right) - c_j\left(c_j^2 + s_j^2\right)^{-1/2} = 0 \\ \dot{s}_j + s_j - c_j\Omega\left(\omega_j - \omega_o\right) - c_j\left(c_j^2 + s_j^2\right)^{-1/2} = 0 \end{cases} \tag{29}$$

and the PSM equations (23) must be updated.

As far as (24) is concerned, if the constant c_o is adopted, the equations ruling the $j-$th machine read

$$\begin{cases} \dot{c}_j + (c_j + c_o) + s_j\Omega\left(\omega_j - \omega_o\right) + \\ \qquad\qquad -(c_j + c_o)\left[(c_j + c_o)^2 + s_j^2\right]^{-1/2} = 0 \\ \dot{s}_j + s_j - s_j\Omega\left(\omega_j - \omega_o\right) - s_j\left[(c_j + c_o)^2 + s_j^2\right]^{-1/2} = 0 \end{cases} . \tag{30}$$

REFERENCES

[1] E. H. Abed and P. P. Varaiya, "Nonlinear Oscillations in Power Systems," *International Journal of Electrical Power and Energy Systems*, vol. 6, pp. 37–43, 1984.

[2] J. C. Alexander, "Oscillatory Solution of a Model System of Nonlinear Swing Equation," *International Journal of Electrical Power and Energy Systems*, vol. 8, pp. 130–136, 1986.

[3] Y. Mitani and K. Tsuji, "Bifurcations Associated with Sub-Synchrouous Resonance," *IEEE Transactions on Power Systems*, vol. 13, no. 1, pp. 139–144, 1998.

[4] I. A. Hiskens, "Stability of Limit Cycles in Hybrid Systems," in *Proceedings of the 34th Hawaii International Conference on System Sciences*, Jan. 2001, pp. 1–6.

[5] B. Nomikos, E. Potamianakis, and C. Vournas, "Oscillatory stability and limit cycle in an autonomous system with wind generation," in *Power Tech, 2005 IEEE Russia*, June 2005, pp. 1–6.

[6] I. Dobson, F. Alvarado, and C. L.DeMarco, "Sensitivity of Hopf Bifurcation to Power System Parameters," *IEEE Decision and Control*, vol. 3, pp. 2928–2933, 1992.

[7] C. A. Cañizares and S. Hranilovic, "Transcritical and Hopf Bifurcation in AC/DC Systems," in *Proceedings of the Bulk Power System Voltage Phenomena III - Seminar*, Davos, Switzerland, Aug. 1994, pp. 105–114.

[8] S. K. Joshi and S. C. Srivastava, "Estimation of Closest Hopf Bifurcation in Electric Power System," in *12th Power System Computational Conference*, Aug. 1996, pp. 195–200.

[9] M. J. Lautenberg, M. A. Pai, and K. R. Padiyar, "Hopf Bifurcation Control in Power System with Static Var Compensators," *International Journal of Electrical Power and Energy Systems*, vol. 19, no. 5, pp. 339–347, Jun. 1997.

[10] O. Nastov, R. Telichevesky, K. Kundert, and J. White, "Fundamentals of fast simulation algorithms for RF circuits," *Proceedings of the IEEE*, vol. 95, no. 3, pp. 600–621, march 2007.

[11] A. Suarez, *Analysis and Design of Autonomous Microwave Circuits*, ser. Wiley Series in Microwave and Optical Engineering. John Wiley & Sons, 2009.

[12] F. Traversa and F. Bonani, "Improved harmonic balance implementation of floquet analysis for nonlinear circuit simulation," *AEU - International Journal of Electronics and Communications*, vol. 66, no. 5, pp. 357–363, 2012.

[13] B. Wang and E. Ngoya, "Integer-N PLLs verification methodology: Large signal steady state and noise analysis," *Circuits and Systems I: Regular Papers, IEEE Transactions on*, vol. 59, no. 11, pp. 2738–2748, Nov 2012.

[14] E. Abed and P. Varaiya, "Nonlinear oscillations in power systems," *International Journal of Electrical Power & Energy Systems*, vol. 6, no. 1, pp. 37–43, 1984.

[15] V. Ajjarapu and B. Lee, "Nonlinear oscillations and voltage collapse phenomenon in electrical power system," in *Power Symposium, 1990., Proceedings of the Twenty-Second Annual North American*, Oct 1990, pp. 274–282.

[16] M. J. Laufenberg, M. Pai, and K. Padiyar, "Hopf bifurcation control in power systems with static var compensators," *International Journal of Electrical Power & Energy Systems*, vol. 19, no. 5, pp. 339–347, 1997.

[17] F. Howell and V. Venkatasubramanian, "Transient stability assessment with unstable limit cycle approximation," *Power Systems, IEEE Transactions on*, vol. 14, no. 2, pp. 667–677, may 1999.

[18] J. Li and V. Venkatasubramanian, "Study of unstable limit cycles in power system models," in *Power Engineering Society Summer Meeting, 2000. IEEE*, vol. 2, 2000, pp. 842–847.

[19] J. Chow, F. Wu, and J. Momoh, "Applied mathematics for restructured electric power systems," in *Applied Mathematics for Restructured Electric Power Systems*, ser. Power Electronics and Power Systems, J. Chow, F. Wu, and J. Momoh, Eds. Springer US, 2005, pp. 1–9.

[20] V. Venkatasubramanian and Y. Li, "Computation of unstable limit cycles in large-scale power system models," in *Circuits and Systems, 2006. ISCAS 2006. Proceedings. 2006 IEEE International Symposium on*, may 2006, pp. 735–738.

[21] T. Aprille and T. Trick, "Steady-state analysis of nonlinear circuits with periodic inputs," *Proceedings of the IEEE*, vol. 60, pp. 108–114, Jan 1972.

[22] ——, "A computer algorithm to determine the steady-state response of nonlinear oscillators," *Circuit Theory, IEEE Transactions on*, vol. 19, no. 4, pp. 354–360, jul 1972.

[23] F. Bizzarri, A. Brambilla, G. Gruosso, and G. Gajani, "Time domain probe insertion to find steady state of strongly nonlinear high-q oscillators," in *Circuits and Systems (ISCAS), 2013 IEEE International Symposium on*, 2013, pp. 1865–1868.

[24] ——, "Probe based shooting method to find stable and unstable limit cycles of strongly nonlinear high-q oscillators," *Circuits and Systems I: Regular Papers, IEEE Transactions on*, vol. 60, no. 7, pp. 1870–1880, 2013.

[25] Y. A. Kuznetsov, *Elements of Applied Bifurcation Theory*, 3rd ed. New York: Springer-Verlag, 2004.

[26] M. Farkas, *Periodic motions*. New York, NY, USA: Springer-Verlag New York, Inc., 1994.

[27] A. Ben-Israel and T. Greville, *Generalized Inverses: Theory and Applications*, ser. CMS Books in Mathematics. Springer, 2003.

[28] F. Milano, *Power System Modelling and Scripting*. Springer Berlin Heidelberg, 2010.

[29] A. Mees, *Dynamics of feedback systems*, ser. A Wiley-Interscience publication. J. Wiley, 1981.

[30] T. S. Parker and L. O. Chua, *Practical Numerical Algorithms for Chaotic Systems*. New York: Springer-Verlag, 1989.

[31] E. Ngoya, A. Surez, R. Sommet, and R. Qur, "Steady state analysis of free or forced oscillators by harmonic balance and stability investigation of periodic and quasi-periodic regimes," *International Journal of Microwave and Millimeter-Wave Computer-Aided Engineering*, vol. 5, no. 3, pp. 210–223, 1995.

[32] M. Gourary, S. Ulyanov, M. Zharov, S. Rusakov, K. Gullapalli, and B. Mulvaney, "Simulation of high-q oscillators," in *Computer-Aided Design, 1998. ICCAD 98. Digest of Technical Papers. 1998 IEEE/ACM International Conference on*, Nov 1998, pp. 162–169.

[33] A. Brambilla, G. Gruosso, and G. Gajani, "Robust harmonic-probe method for the simulation of oscillators," *Circuits and Systems I: Regular Papers, IEEE Transactions on*, vol. 57, no. 9, pp. 2531–2541, Sept 2010.

[34] L. Petzold, S. Li, Y. Cao, and R. Serban, "Sensitivity analysis of differential-algebraic equations and partial differential equations," *Computers & Chemical Engineering*, vol. 30, no. 10, pp. 1553–1559, 2006.

[35] P. Sauer and M. A. Pai, "Power system steady-state stability and the load-flow jacobian," *Power Systems, IEEE Transactions on*, vol. 5, no. 4, pp. 1374–1383, Nov 1990.

[36] B. Aulbach, *Continuous and Discrete Dynamics Near Manifolds of Equilibria*, ser. Lecture Notes in Mathematics. Springer-Verlag, 1984.

[37] ——, "Behavior of solutions near manifolds of periodic solutions," *Journal of Differential Equations*, vol. 39, no. 3, pp. 345–377, 1981.

[38] F. Bizzarri, A. Brambilla, G. Storti Gajani, and S. Banerjee, "Simulation of real world circuits: Extending conventional analysis methods to circuits described by heterogeneous languages," *IEEE Circuits and Systems Magazine*, vol. 14, no. 4, pp. 51–70, 2014.

[39] M. Powell, *A Hybrid Method for Nonlinear Equations (Chap 6, pp. 87–114) and A Fortran Subroutine for Solving systems of Nonlinear Algebraic Equations (Chap 7, pp. 115–161) in Numerical Methods for Nonlinear Algebraic Equations*. P. Rabinowitz, editor. Gordon and Breach, 1970.

[40] P. W. Sauer and M. A. Pai, *Power System Dynamics and Stability*. Upper Saddle River, New Jersey: Prentice Hall, 1998.

[41] A. Brambilla and G. Storti-Gajani, "Frequency warping in time domain circuit simulation," *IEEE Transactions on Circuits and Systems I: Fundamental Theory and Applications*, vol. 50, pp. 904–913, July 2003.

Federico Bizzarri (M'12, SM'14) was born in Genoa, Italy, in 1974. He received the Laurea (M.Sc.) five-year degree (summa cum laude) in electronic engineering and the Ph.D. degree in electrical engineering from the University of Genoa, Genoa, Italy, in 1998 and 2001, respectively.

Since June 2010 he has been a temporary research contract assistant professor at the Electronic and Information Department of the Politecnico di Milano, Milan, Italy. In 2000 he was a visitor to EPFL, Lausanne, Switzerland. From 2002 to 2008 he had been a post-doctoral research assistant in the Biophysical and Electronic Engineering Department of the University of Genova, Italy. In 2009 he was a post-doctoral research assistant in Advanced Research Center on Electronic Systems for Information and Communication Technologies "E. De Castro" (ARCES) at the University of Bologna, Italy.

His main research interests are in the area of nonlinear circuits, with emphasis on chaotic dynamics and bifurcation theory, circuit models of nonlinear systems, image processing, circuit theory and simulation. He is the author or coauthor of about 80 scientific papers, more than an half of which have been published in international journals. He is a research fellow of the Advanced Research Center on Electronic Systems for Information and Communication Technologies "E. De Castro" (ARCES) at the University of Bologna, Italy.

Since 2012 he is serving as an Associate Editor of the IEEE Transactions on Circuits and Systems — Part I and he was awarded as one of the 2012-2013 Best Associate Editors of this journal. In 2103, 2015 and 2016, he has been a member of the Review Committee for the Nonlinear Circuits and Systems track at the IEEE International Symposium on Circuits and Systems.

Angelo Brambilla (M'16) received the Dr. Ing. degree (summa cum laude) in electronics engineering from the University of Pavia, Pavia, Italy, in 1986. Currently he is full professor at the Dipartimento di Elettronica, Informazione e Bioingegneria, Politecnico di Milano, Milano, Italy, where he has been working in the areas of circuit analysis and simulation. In 2008-2010 he served as AE for TCAS-II.

Federico Milano (S'02, M'04, SM'09, F'16) received from the Univ. of Genoa, Italy, the ME and Ph.D. in Electrical Eng. in 1999 and 2003, respectively. From 2001 to 2002 he was with the Univ. of Waterloo, Canada, as a Visiting Scholar. From 2003 to 2013, he was with the Univ. of Castilla-La Mancha, Spain. In 2013, he joined the Univ. College Dublin, Ireland, where he is currently an associate professor. His research interests include power system modelling, stability analysis and control.